Nebulizing novel multifunctional nanovesicles: the impact of macrophage-targeted-pH-sensitive archaeosomes on pulmonary surfactant

Maria Julia Altube[1], Andrea Cutro[2], Laura Bakas[3], Maria Jose Morilla[1], Edgardo Anibal Disalvo[2] and Eder Lilia Romero[1]

[1] Nanomedicine Research Program-2, Science and Technology Department, National University of Quilmes, Bernal, Buenos Aires, Argentina

[2] Laboratory of Biointerphases and Biomimetic Systems, (CITSE) National University of Santiago del Estero and CONICET, 4206, RN 9- Km 1125, Santiago del Estero, Argentina.

[3] Vegetal Proteins Research Laboratory (LIPROVE), Exact Sciences Faculty, National University of La Plata, Buenos Aires, Argentina

Abstract

In this work, a NE-U22 vibrating mesh Omron nebulizer was used to deliver Rh-PE and HPTS/ DPX double labelled macrophage-targeted pH-sensitive archaeosomes (ApH, 174 ± 48 nm, - 30 ± 13 mV unilamellar nanovesicles made of dioleoyl-sn-glycero-3-phosphoethanolamine: [total polar archaeolipids from the hyperhalophile archaebacteria *Halorubrum tebenquichense*]: cholesterylhemisuccinate 4.2:2.8:3 w:w:w) - on J774A1 cells covered by Prosurf pulmonary surfactant (PS) monolayer at or below the equilibrium surface pressure πe. The uptake and cytoplasmic drug release from ApH were assessed by flow cytometry of Rh-PE and HPTS fluorescence respectively. Despite of being soft matter submitted to dismantling interactions of shear stress of nebulization and contact with surfactant barrier, at least a fraction of nebulized ApH was found to be stable enough to execute higher cytoplasmic delivery than archaeolipids lacking vesicles.

Nebulized ApH increased the PS tensioactivity below πe only, out of the physiological range. This would mean that *in vivo*, changes in lung surfactant function induced by nebulized nanovesicles, is poorly likely to occur. The cytoplasmic delivery from ApH slightly decreased across monolayers at πe , suggesting that nanovesicles crossed the PS in a fashion inversely related to monolayer compression. Laurdan Generalized Polarization and Fluorescence Anisotropy were used to reveal that nanovesicles neither depleted B and C proteins of the PS, not increased its fluidity. Together with the feasibility of cytoplasmic drug delivery upon nebulization, our results suggest that ApH are structurally unique nanovesicles that would not induce biophysical changes leading to PS inactivation, and open the door to future deeper translational studies.

1 Introduction

Inhalation of therapeutic nanoparticles is at the edge of clinical implementation. Unlike parenteral delivery, inhalation is a non-invasive route, may localise the drug action in the lung for prolonged periods and may reduce systemic adverse effects. [1,2,3] Worth to note however, that from the wide range of structural types of nanoparticles developed so far, and because of their robust methods of production and high biocompatibility [4], only lipid nanovesicles, followed by polymeric micelles and nanocrystals, fit into the selected portfolio of the pharmaceutical industry. [5,6] If well nanovesicles in clinical use are mostly intended for parenteral administration, inhalation of aqueous suspension of nanovesicles is preferentially carried out employing nebulizers. The output of the nebulizers in terms of liposomal transport efficiencies differed significantly among the nebulizer principles (20–100%, $p < 0.05$), with the vibrating-mesh nebulizers being the most effective.[7]Compared to other inhalation devices, nebulisers can generate large volumes of 'respirable' aerosol, with no need to perform drying procedures, as in the case of dry powder inhalers, or involve propellants, as in case of pressured metered dose inhalers.[1] Three nebulizable nanovesicule formulations: liposomal ciprofloxacin (Pulmaquin ® and Lipoquin®) and liposomal amikacyne (Arikace ®) are in current advanced clinical studies.[8,9] Up to now a solid knowledge on pharmacotechnical, preclinical and clinical features has been documented on these future pharmaceutical products. However, scarce biophysical studies aimed to unravel their interaction with PS have been performed.

Recently, we have described the structural features of pH-sensitive archaeosomes (ApH), nanovesicles displaying key properties expected to speed future industrial translation.[10,11]The ApH are multifunctional nanovesicles offering a versatile platform for drug delivery because of their archaeolipids content. The archaeolipids are novel biomaterials extracted from a non-conventional (neither animal, vegetal not bacterial) source, the hyperhalophile archaebacteria *Halorubrum tebenquichense*. The presence of such archaeolipids, particularly of the majoritarian component PGP-Me (Fig 1), renders the nanovesicles resistant to physical, chemical and enzymatic attacks, including to shear stress of nebulization. The ApH combine two characteristics needed to achieve massive drug delivery to the cell cytoplasm: a) high endocytic uptake rate, owed to the presence of archaeolipids, that are ligands of the class A scavenger receptors[10] and enable specific macrophages and vascular endothelial cells targeting, avoiding the use of covalent derivatization [12] and b) ability to respond to endosomal acidity with a phase transition, subsequent fusion between endosome and ApH bilayers, and massive inner content release to cell cytoplasm, owed to its DOPE:CHEMS content. ApH also surpasses the ability of ordinary (archaeolipids lacking) pH-sensitive nanovesicles (LpH), in releasing hydro soluble drugs to the cell cytoplasm. Because of that, while higher doses of free or loaded in other nanovesicles dexamethasone phosphate failed, a small amount of dexamethasone-loaded in ApH was sufficient to *in vitro* efficiently reduce a strong inflammatory response elicited by lipopolysaccharide in macrophages (J774A.1 and THP-1).[10]

ApH display also a superior structural endurance compared to LpH: where these last are dismantled, the colloidal structure of ApH is retained upon at least six months of storage in aqueous media and further nebulization employing vibrating mesh technology. Nebulizable (non-pH-sensitive) nanovesicles require of cholesterol or hydrogenated phospholipids to make bilayers resistant to shear stress and chemical attacks.[8,13] Hydrogenated phosphatidylcholine however, is expensive and may be contaminated with highly toxic *trans* isomers.[14]In ApH the hydrogenated phosphatidylcholine is replaced by polar archaeolipids that grant structural stability during storage and subsequent nebulization.[10,11]

More specifically, nebulizable ApH are aimed to target alveolar macrophages, immune cells living under the air-blood interface, covered by a thin film of pulmonary surfactant (PS).[15]The PS interposes between all respirable nanoparticles, and target cells in the alveoli. The PS holds at least three essential biophysical properties for normal respiratory physiology. They are rapid adsorption, very low surface tension on film compression, and effective film replenishment on film expansion.[16] Thus, when thinking of respirable nanoparticles formulations, these have not only to survive to nebulization stress, storage, and targeted drug delivery after crossing a detergent monolayer, but also to grant safety for the respiratory function. Surfactant inactivation is life-threatening and refers to all processes that interfere with and decrease surface activity of

surfactant. PS inactivation may occur because of external (leakage of surface active serum proteins, meconium, fatty acids, lysoderivatives, protein C reactive) or endogenous (altered secretion by alveolar type II cells) factors.[17] The advent of new techniques for detection, production and structural characterization of respirable nanoparticles, enabled to survey their impact on respiratory function, specifically of their interaction with PS.[18,19] The role of PS is to facilitate the respiratory dynamics by diminishing the water surface tension at the alveolar interfase.[17,20] An ample evidence have emerged supporting the fact however, that translocation of polymeric, silicon oxide pristine or methylated, titania oxide[21], negatively- and positively-charged poly(styrene)[22] or metallic nanoparticles, induces PS inactivation**.** Hydroxyapatite nanoparticles injected into PS Infasurf subphase for instance, cause a significant time dependent shift of compression isotherms to the left, i.e., more area reduction is required to increase surface pressure, indicating surfactant inactivation.[23]Nanoparticles in contact with lung surfactant must prove therefore, not to induce surfactant inactivation.

In this work, the cytoplasmic drug release of pH-sensitive nanovesicles nebulized on a Prosurf (a PS obtained from a bovine/porcine lung lavage and having cholesterol, hydrophobic B and C proteins and phospholipids) monolayer covering J774A.1 cells, was determined. The study was complemented with a survey of the effect of subphase injected or nebulized nanovesicles, on the surface pressure of a Prosurf monolayer. Here we report for the first time that nebulized nanovesicles remained structurally stable after crossing the PS monolayer. After passage, nebulized nanovesicles could efficiently release a cytoplasmic fluorophore marker into the underlying cells. We also found that upon injected in the subphase, or after nebulized, the surface pressure of Prosurf was increased by the presence of ApH. Despite of being more efficiently induced by nebulization, such effect occurred at very low surface pressure, out of the physiological compression expansion range. Overall, such findings suggest that nebulized nanovesicles used in this work are not expected to induce biophysical changes leading to PS inactivation, opening the door to future deeper translational studies.

2 Materials and methods

2.1 Materials

Pulmonary surfactant (PS) Prosurf was a gift from Nialtec S.A. (Buenos Aires, Argentina). Soybean phosphatidylcholine (SPC, purity>90%) was a gift from Lipoid (Ludwigshafen, Germany). 1,2-Hydrogenated-L-α-phosphatidylcholine (HSPC) was from Northern Lipids Inc (Vancouver, Canada); Dioleoyl-sn-glycero-3-phosphoethanolamine (DOPE) was from Avanti Polar Lipids (Alabama, USA); p-xylene-bis-pyridinium bromide (DPX) was from Invitrogen (Oregon, USA). Cholesterol, cholesteryl hemisuccinate (CHEMS), 8-Hydroxypyrene-1,3,6-trisulfonic acid trisodium salt (HPTS), Laurdan, Sephadex® G-25 Fine were from Sigma Aldrich (Missouri, USA). Lissamine™ rhodamine B 1,2-dihexadecanoyl-sn-glycero-3-phosphoethanolamine triethylammonium salt (RhPE) was purchased from Thermo Fisher Scientific (Massachusetts, USA). Roswell Park Memorial Institute (RPMI) 1640, penicillin-streptomycin sulphate and glutamine were from Gibco®, Life Technologies (New York, USA); fetal bovine serum (FBS) was from Internegocios (Cordoba, Argentina). The other reagents were analytic grade from Anedra, Research AG (Buenos Aires, Argentina).

2.2 Archaebacteria growth, extraction, and characterization of total polar archaeolipids

Halorubrum tebenquichense archaeabacteria, isolated from soil samples of Salina Chica, Península de Valdés, Chubut, Argentina were grown in basal medium supplemented with yeast extract and glucose at 37°C.[24] Biomass was grown in 15 L medium in a 25 L home-made stainless steel bioreactor and harvested after 96 h growth. Total polar archaeolipids (TPA) were extracted from biomass using the Bligh and Dyer method modified for extreme halophiles.[25] Between 400 mg and 700 mg TPA were isolated from each culture batch. The quali-quantititive composition of each TPA extract was routinely screened by phosphate content[26] and electrospray-ionization mass spectrometry.[27]

2.3 Preparation of nanovesicles

Conventional nanovesicles made of HSPC:cholesterol 9:3 w:w (L), archaeosomes made of TPA (ARC), pH-sensitive nanovesicles made of DOPE:CHEMS 7:3 w:w (LpH) and pH-sensitive archaeosomes made of DOPE:TPA:CHEMS 4.2:2.8:3 w:w (ApH); were prepared by

the film hydration method, as described in Altube et al.[10] Briefly, mixtures of lipids were dissolved in chloroform: methanol 1:1 v:v; solvents were rotary evaporated at 40°C until elimination. The lipid films were flushed with N_2 and hydrated with aqueous phase (10 mM Tris-HCl buffer pH 7.4 with 0.9 % w:w NaCl -Tris-HCl buffer) up to a final concentration of 10 mg/mL total lipids. The resultant suspensions were sonicated (1 hour with a bath-type sonicator 80 W, 80 KHz) and extruded 21 times through 0.2 µm pore size polycarbonate filters using a manual extruder (Avanti PolarLipids, Alabama, USA). The resulting nanovesicles were sterilized by passage through a 0.22 µm sterile filter, and stored at 4°C.

2.4 Preparation of PS vesicles

Prosurf is a sterile chloroform solution that contains lipids and proteins extracted by means of bronchoalveolar lavage from bovine lungs. Prosurf is composed of phospholipids (PL) 94.8% (which dipalmitoylphosphatidylcholine (DPPC) is 46%); cholesterol 4.4% and proteins (SP-B, SP-C) 0.8%.[28] Chloroform was evaporated at low pressure and below 40°C; the film was resuspended in sterile saline solution (0.9% NaCl) at 50°C, obtaining a final phospholipid concentration of 30 mg/mL, corresponding to 41 mM DPPC (PS vesicles).

2.5 Quantification of phospholipids

Phospholipids were quantified by a colorimetric phosphate microassay.[26]

2.6 Size and Z potential

Size and Zeta potential of nanovesicles and PS vesicles were determined by dynamic light scattering (DLS) and phase analysis light scattering (PALS) respectively, using a nanoZsizer apparatus (Malvern Instruments, Malvern, United Kingdom).

2.7 Preparation of HPTS/DPX and RhPE labelled nanovesicles

To prepare HPTS/DPX labelled nanovesicles (HPTS/DPX-nanovesicles), lipid films were hydrated with 35 mM HPTS and 50 mM DPX in Tris-HCl buffer. Free HPTS and DPX were removed from HPTS/DPX-nanovesicles by gel filtration on Sephadex G-25 using the minicolumn centrifugation technique.[10]To prepare double-labelled nanovesicles (RhPE and HPTS/DPX), RhPE was added at 0.5% weight to the organic lipid solutions and lipid films were hydrated with HPTS–DPX solution as stated above.

RhPE was quantified by spectrofluorometry (λ_{ex} =561 nm and λ_{em} = 580 nm) with a Fluorescence Spectrometer LS Perkin Elmer, upon complete disruption of 1 volume of nanovesicles in 40 volumes of methanol. The fluorescence intensity (I) of the sample was compared with a standard curve prepared with RhPE in methanol. The standard curve was linear in the range 0.075–0.5 µg/mL RhPE with a correlation coefficient of 0.999.

HPTS was also quantified by spectrofluorometry (λ_{ex} = 413 nm and λ_{em} = 515 nm) before and after complete disruption of 1 volume of nanovesicles in 175 volumes of Tris-HCl buffer with Triton X-100 1% w/v. The fluorescence intensity (I) of the sample, calculated as I with Triton X-100 - I without disruption, was compared with a standard curve prepared with HPTS–DPX in solution. The standard curve was linear in the range 0.18–12 µM HPTS with a correlation coefficient of 0.996.

2.8 J774A.1 cells growth

Immortalized murine Balb/c macrophages J774A.1 (ATCC® TIB-67™), supplied by Dr Erina Petrera (Facultad de Ciencias Exactas y Naturales, Universidad Nacional de Buenos Aires Argentina), were maintained in RMPI 1640 supplemented with 10% FBS, 100 U/mL penicillin, 100 µg/mL streptomycin and 2 mM L-glutamine (complete RMPI medium) in a humidified atmosphere of 5% CO_2 at 37°C.

2.9 Nebulization of HPTS/DPX-RhPE nanovesicles on J774A.1 cells covered by PS monolayers

Briefly, J774A.1 cells were seeded on 24-well culture plates at a density of 1.5×10^5 cells per well. Upon 24 h growth, the culture media was removed and replaced by 300 µLphosphate-buffered saline (PBS). A chloroform solution of PS (3.1 mg / mL) was spread on the aqueous interface of PBS up to 10 ± 1 mN / m or 45 ± 1 mN / m π, a value close to πe, the equilibrium surface pressure of phosphatidylcholines. πe is the maximum surface pressure of compressed monomolecular films at an air/water interface under equilibrium conditions. A further compression induces the collapse of the two-dimensional interface, to form three-dimensional structures[29,30], but no increase in the density of the monolayer or in surface pressure occurs.[31,32]A NE-U22

vibrating mesh Omron nebulizer, adapted to reduce the output flow at5 µL/ min rate, was used to nebulize aqueous suspensions of nanovesicles at 2.5 mg/mL total lipids on the surface of each Prosurf monolayer for 1 minute. Cells were incubated for 3 h at 37°C, washed, trypsinized, resuspended in phosphate-buffered saline (PBS) and a total of 1×10^4 cells were analysed by flow cytometry. For HPTS, green fluorescence (FL-1) was analysed, whereas for RhPE the red fluorescence (FL-3) was analysed. The fluorescence was further normalized to the HPTS /total lipids and RhPE /total lipids ratio of each formulation. The colloidal stability of nanovesicles nebulized across the PS monolayer, before being taken up by underlying cells, was determined by measuring the % encapsulated HPTS upon extracted from cell supernatants 3 h after nebulization. The uptake and subcellular pH-sensitivity of double labelled RhPE–HPTS/DPX-nanovesicles was followed by the fluorescence of rhodamine, while the fluorescence of HPTS indicated its degree of subcellular dequenching, or pH-sensitivity.[10]

2.10 Mutual bilayer perturbation of PS vesicles and nanovesicles:

2.10.1 Laurdan generalized polarization (GP) and fluorescence anisotropy (FA) of PS vesicles

The order and fluidity of PS bilayer upon contacting nanovesicles, were assessed by determining GP and FA respectively, of Laurdan in PS vesicles.

PS vesicles were labelled with Laurdan by mixing 10 µL of 120 mM Laurdan in methanol with a volume of PS vesicles sufficient to render a 1:20 mol:mol Laurdan:lipids. After 30 minutes, nanovesicles were added at 1:0.1 PS vesicles: nanovesicles w: w ratio; the mixture was incubated at room temperature. GP, FA of PS vesicles bilayers and size were determined as a function of time.

GP was calculated using the following equation:

$GP = I_{440} - I_{490} / I_{440} + I_{490}$

Where I_{440} and I_{490} are the fluorescence intensities at λ_{em} =440 nm and λ_{em} =490 nm respectively and obtained from the spectra between 400-520 nm at λ_{ex} =364nm (Slit $_{ex}$:5.0 nm and Slit $_{em}$: 10.0 nm. Scan Speed: 100 nm/min)

FA was calculated by the fluorimeter software according to the following equation:

$FA = (I_0 - G\, I_{90}) / (I_0 + 2G\, I_{90})$

Where I_0 and I_{90} are the fluorescence intensities at λ_{em}=440 nm with λ_{ex} = 364 nm and the excitation polarizer oriented at 0 and 90° respectively. The correction factor (G) was obtained from the ratio of emission intensity at 0 and 90° with the excitation polarizer oriented at 90°(after subtraction of scattered light).

2.10.2 Laurdan GP and FA of nanovesicles

Similarly, the order and fluidity of nanovesicles bilayers upon contacting PS vesicles were assessed by GP and FA respectively, of Laurdan in nanovesicles, employing the same experimental conditions than in **2.12.1**

2.10.3 Inner content leakage of nanovesicles

The HPTS released from HPTS/DPX-nanovesicles upon contacting PS vesicles, was determined as a function of time. Briefly, HPTS-DPX-nanovesicles were incubated 1, 5 and 20 h at 25°C in 10 mMTris-HCl buffer with PS vesicles at the same ratio than in **2.10.1**. The percentage of released HPTS was calculated as follows: $(I / I_{Triton\ X\text{-}100}) \times 100$. Where I is the fluorescence intensity at λ_{em}= 515 nm and λ_{ex}=413 nm at each time point, and $I_{Triton\ X\text{-}100}$ is the fluorescence intensity after adding 1% w/v Triton X-100.

In addition, the average size of nanoliposome and PS vesicles was determined by DLS.

2.11 Effect of nanovesicles on surface pressure (π) during compression-expansion cycles

The surface pressure π is defined as the extent to which a film reduces the surface tension of a clean interface; it denotes the two-dimensional equivalent of pressure in three dimensions, or the force exerted by an interfacial film on its linear confining boundaries, with units of force/length.[33]Surface pressure vs area (π *vs* A) isotherms were run in the KSV trough (240 cm^2 area) of a Wilhelmy balance provided by a Platinum probe (39.24 mm^2) (KSV-NIMA, Finland). The whole equipment was enclosed in an acrylic box to minimize solvent evaporation and to avoid contaminations from the environment during the study. A compression isotherm for the Prosurf monolayer was first determined. To that aim, a PS monolayer was prepared by spreading a chloroform solution of PS (3.1 mg / mL) on the aqueous interface of 10 mM Tris-HCl buffer and

allowed to stabilize during 30 min. after that, the monolayer was submitted to a 5 mm/min compression rate.

Compression and expansion rate of PS monolayers were performed at 5 mm/min, target pressure π was set at 30 mN/m (compression) and 1 mN/m (expansion) and the temperature was 20 ± 2 °C. Nanovesicles were injected into the subphase at a final concentration of 10 μg/mL at 30 mN/m π at the end of the first compression. After each measure, the KSV trough was exhaustively cleaned with pure water and the surface tension was verified to be 72 mN/m. The surface pressure and the barriers were controlled by software purchased from NIMA (KSV-NIMA, Finland). Control experiments in the absence of nanovesicles were also carried out in the same conditions, spreading the same amount of PS on the surface.

2.12 Effect of nanovesicles on π at constant area:

2.12.1 Nanovesicles injected in the aqueous subphase

A chloroform solution of PS (3.1 mg / mL) was spread on the aqueous interface of 10 mM Tris-HCl buffer in order to attain an initial pressure of 10 ± 1 mN / m, 30 ± 1 mN / m and 45 ± 1 mN / m π respectively, in a Kibron μtrough S equipment (13.6 cm^2 area, 8 mL subphase) (Kibron, Finland). The changes in surface pressure of PS monolayer upon injection of nanovesicles into the subphase were registered as a function of time, until a constant pressure value was reached. The final concentration of injected nanovesicleswere 0.3 and 10 μg/mL, respectively.

In order to avoid the solvent evaporation and contamination from the environment during the study, the whole equipment was enclosed in an acrylic box. After each measure, the trough was exhaustively cleaned with pure water and the surface tension was verified to be 72 mN/m. In all the assays, the temperature was maintained at 20 ± 0.5 ° C

2.12.2 Nebulized nanovesicles

Employing identical conditions than in **2.11.1,** nanovesicles were first nebulized for 1 minute, followed by a second dose 15 minutes later at 0.06 or 1.5 μg total doses; after that the monolayer was allowed to stabilize other 15 minutes.

2.13 Statistical analysis

Statistical analyses were performed by one-way analysis of variance followed by Dunnet's test using Prisma 6.0 Software (Graph Pad, CA, USA). The p-value of <0.05 was considered statistically significant. *p < 0.05; **p < 0.01; ***p < 0.001; ****p < 0.0001; n.s. represents non-significant (p > 0.05).

3 Results

3.1 Compression isotherm of Prosurf and structural features of nanovesicles

The compression isotherm of the lung surfactant Prosurf employed in this work, showed a collapse pressure (π_c) of ~ 60 mN/m (Fig. 2), a value closer to the π_c of bovine derived clinical surfactant Survanta (Abbott Laboratories, North Chicago, IL) (62 mN/m) than to the porcine derived Curosurf (CHIESIUSA.com), or bovine derived Infasurf (ONYINC), which are nearly 10 mN/M higher.[34]The structural features of nanovesicles are depicted in Table 1.

3.2 Uptake of nebulized nanovesicles and cytoplasmic delivery on J774A.1 macrophages under a PS monolayer

As already reported, the shear stress of nebulization induced a partial loss of aqueous content from nanoliposomes.[10] As depicted in Table 2 however, nanoliposomes lost nearly the half excepting ApH, that retained nearly 75 % of its aqueous content. After crossing the PS monolayers however, no further loss of HPTS occurred: after nebulized on buffer or on PS monolayers at 10 or 45 mN/m, the amount of retained HPTS remained identical. On the other hand, after crossing the PS monolayers covering underlying J774A.1 cells, we observed that archaeolipid-containing nanovesicles ARC and ApH, were up taken in the highest extent (highest RhPE signal), followed by LpH, while no uptake of L was registered (Fig. 3a). In agreement with our previous report on cytoplasmic delivery by ApH (on cells uncovered by a PS monolayer)[10], ApH displayed again the highest cytoplasmic delivery, as measured by the highest intensity of the HPTS signal. ARC, while it was up taken in equal extent than ApH, did not release its aqueous content (HPTS) to the cell cytoplasm, because of its lack of pH-sensitivity. It was also observed that, at 45 mN/m (a value close to πe of phosphatidylcholines) the uptake and subsequent cytoplasmic delivery of ApH seemed to slightly decline, as compared to that at 0 or 10 mN/m (Fig.

3b). Overall, we observed that at least a fraction of nebulized nanovesicles spanned the PS monolayer in intact form. After entering the subphase, the nanovesicles were captured by underlying cells and processedaccording to the structural characteristic of each other. The slightly decreased uptake and subsequent cytoplasmic delivery at πe suggests that during the respiratory cycle, the uptake of nebulized nanovesicles would follow an inverse relationship with surface pressure, being probably lower when the PS monolayer is fully compressed well aboveπe.

3.3 Mutual bilayer perturbation of PS vesicles and nanovesicles

Laurdan is a fluorescent probe of membrane structure, sensitive to the solvent relaxation effect. The dye senses the differences in number/mobility of water molecules associated to the phospholipid glycerol backbone of phosphatidylcholine bilayers.[22,37,38] Upon excitation, the dipole moment of Laurdan increases noticeably, and water molecules in the vicinity of the probe reorient around this new dipole. Accordingly, Laurdan is sensitive to membrane phase transitions and other alterations to membrane fluidity.[39-40] When the membrane is in a fluid phase, the reorientation rate is faster than the emission process, and consequently, a red-shift at λ_{ex}=340 nm from about 435 nm to about 480 nm is observed.[39]When the bilayer packing increases, some of the water molecules are excluded from the bilayer, and the dipolar relaxation rate of the remaining water molecules is slower, leading to an emission spectrum that is significantly less red-shifted. The generalized polarization (GP) quantifies this red-shift from the emission spectra. In particular, the work of Harris 2002[41]noticed that when membrane fluidity changes but phospholipid order (defining ‘‘order’’ as representing conformational order of the phospholipid molecules (mostly based on the acyl chains) and “fluidity” as representing the ability of lipids to diffuse in the plane of the bilayer and/or rotate[42] remains constant, one would expect Laurdan fluorescence anisotropy (FA), but not GP, to also change. The change from disordered toward ordered phases represents an actual loss of water molecules from the bilayers. Since FA reports changes in membrane fluidity while GP is more sensitive to variations in membrane order[41], the mutual perturbations in order and fluidity of PS vesicles contacting nanovesicles, were here assessed by Laurdan GP and FA.

3.3.1 GP of PS vesicles: the bilayer order (GP) of PS vesicles and of each nanoliposome alone was: PS vesicles ~L>[ApH~LpH]>> ARC. Upon contact with nanovesicles, the order of PS vesicles (compared to that of PS vesicles alone) was: PS vesicles~[PS vesicles-L]>[PS vesicles-(ApH, LpH)]>[PS vesicles-ARC]. The contact with L did not modify the bilayer order of PS vesicles; ApH and LpH intermediately disordered the PS bilayers, while the highest disorder was induced by ARC (Fig. 4a).

3.3.2 FA of PS vesicles: the bilayer FA (inversely related to fluidity[41]of PS vesicles and of each nanovesicle alone was: PS vesicles~L>ARC>ApH>LpH. Upon contact with nanovesicles, the FA of PS vesicles (compared to that of PS vesicles alone) was: [PS vesicles-L] >PS vesicles ~ [PS vesicles - (ApH, LpH, ARC)]. The contact with L slightly decreased the fluidity of PS vesicles; the reminder nanovesicles had not effect on the fluidity of PS vesicles (Fig. 4b).

3.3.3 GP and FA of nanovesicles: 24 h after contacting PS vesicles on the other hand, the order of pH-sensitive nanovesicles and ARC significantly increased to values close to 0.2 (the GP of PS vesicles alone), while the fluidity of all nanovesicles decreased (Fig. 5).

Briefly, excluding L, nanovesicles had no effect on the fluidity of PS vesicles. However, a mutual perturbation in bilayer order occurred upon contact between PS vesicles and nanovesicles. The highest disorder on PS bilayers was induced by ARC; LpH and ApH induced less disorder while the contact withL had no effect on it. Roughly, the order of PS bilayers seemed to shift towards those values typical for each type of nanoliposome, suggesting the occurrence of a lipid flux from nanovesicles (particularly from ARC) towards PS vesicles. This may be the case of the high disorder in PS bilayers induced by ARC. The archaeolipids are known to form an homogeneous phase with phospholipids.[43] Besides, archaeolipids bilayers exhibit peculiar structural features, different from phospholipid bilayers in that though highly entropic (disordered), display a relatively low permeability and reduced lateral diffusion.[44]FA depends on the viscosity of the local molecular environment, in this case, the bilayer; and is also inversely proportional to the rotational rate of Laurdan, a parameter directly related with bilayer fluidity.[41] The Laurdan GP and FA values of ARC indicated disordered bilayers having highly reduced lateral mobility. PS vesicles and ARC bilayers both exhibit low fluidity (high FA)**.** However, PS vesicles bilayers are highly ordered and become disordered after contacting ARC.

3.3.4 Size change of PS vesicles and inner content leakage of nanovesicles

After HPTS-DPX nanovesicles contacted PS vesicles, the mean size of PS vesicles (shown in Table 1) remained unchanged. Besides, no HPTS release from nanovesicles was recorded.

3.4 Effect of nanovesicles on π during compression-expansion cycles (dynamic condition)

Upon injected in the subphase of PS monolayers, π varied according to each nanoliposome structural type (Fig. 6). The effect of L and ARC was displayed during the second expansion. Between 30 and 0 mN/m (200 cm^2) for L, and ~ 5mN/m (175 cm^2) for ARC, the expansion was almost identical to that of PS alone (Fig. 6a). From these points to the end of the expansion, π did not decrease to 0, but raised to ~5 and ~ 25 mN/m, respectively (Fig. 6b,c).

On the contrary, LpH and ApH immediately affected π along the first expansion. Between 30 mN/mand ~9 mN/m (150 cm^2) forLpH and ~12.5 mN/m (150 cm^2) forApH, the expansion was almost identical to that of PS alone. However, from these points to the end of the expansion, π did not decrease to 0 but raised to ~ 25 mN/m. The second compression required only a reduction in area of 16 % (to ~ 210 cm^2) to raise π from 25 to 30 mN/m (Fig. 6d, e). Instead, PS monolayers alone required a reduction in area of 60 % (from 250 to ~ 100 cm^2), to raise π from 0 to 30 mN/m. This signified that the insertion of pH-sensitive nanovesicles enabled the induction of nearly 4 folds less compression to achieve the maximal value of π.

Overall, these results suggest that pH-sensitive nanovesicles were rapidly adsorbed, to pronouncedly affect π at the relatively high degree of compression of 150 cm^2. ARC and L adsorbed later and on more relaxed monolayers (>175 cm^2). According to their capacity to perturb π, nanovesicles ordered as follows: ApH=LpH>ARC>>L. A direct relationship between their ability for inserting into more compressed monolayers and the increase of π was revealed: while components of pH-sensitive nanovesicles were inserted into more compressed monolayers at 150 cm^2, ARC components did it on less compressed monolayers at (175cm^2) whereas L components required almost fully expanded (200cm^2) monolayers.

3.5 Subphase injection vs nebulization of nanovesicles on PS monolayers (static condition)

Since the interaction between nanovesicles and PS monolayer was observed to start during the expansion, the effect of high (80 μg) and low (2.4 μg) mass of nanovesicles on PS monolayers expanded at a fixed 10 mN/m $\pi$was tested. The effect of 80 μg of pH- sensitive nanovesicles was noted after 15 minutes, with π increasing in a 50 % (LpH) and a 75 % (ApH) (Fig. 7a).

Overall, the effects of injected nanovesicles agreed with previous compression-expansion data: pH-sensitive nanovesicles adsorbed fastest and deeply increased π. According to their capacity to perturb π, nanovesicles ordered as follows: Aph~ Lph> ARC~ L.

In a further step the effect of nebulized nanovesicles was tested on PS monolayers expanded at 10 mN/m. This time it was found that after 15 minutes, 1.5 μg pH-sensitive nanovesicles were sufficient to increase πin a ~ 80 for LpH and a 140 % for ApH. Remarkably, ARC also increased π in a 60%. These results suggested that the nebulization induced a faster spreading, and a more efficient increase of π achieved with ~ 53 folds lower mass than if injected in the subphase (Fig. 7b). According to their capacity to perturb π, the nanovesicles are ordered as follows [similar to that when injected during compression-expansion]: ApH>LpH> ARC>L.

Finally, the effect nebulized nanovesicles on PS monolayers at different degrees of compression was tested. 1.5 μg nanovesicles induced less pronounced increases in PS monolayer at 30 mN/m π, following a trend similar to that on the expanded monolayer. At 45 mN/m however, no changes in π were registered. This can be interpreted as a threshold between 30 and 45 mN/m π, above which the surface-active monomers can no longer be inserted in the monolayer (Fig. 8).

4 Discussion

Nebulized nanovesicles aimed for cytoplasmic drug delivery such as ApH, are expected to be endocytosed in intact form. We had already shown that ApH is partly sensitive to shear stress

of nebulization, since nearly one third of its inner content is lost.[10] Besides, a recent report shows that nebulization induces the loss of lipid monomers from nanovesicles bilayer, a fact potentially leading to hydrophilic content loss.[45] Up to now, no data on the fate of nebulized nanovesicles across a PS is available. The combination of shear stress of nebulization, with the potential physical PS barrier encountered by nebulized ApH, may led to reduce or even to eliminate the amount of intact ApH gaining access the underlying cells.

In the first section of this work, we showed that a fraction of nanovesicles survived nebulization and subsequent spanning of the PS monolayer, still efficiently delivering their cargo to underlying macrophages cytoplasm.

Secondly, a few basic biophysical determinations, aimed to characterize the interaction between PS and nanovesicles to predict the occurrence of a potential surfactant inactivation, were performed. In first place, size, order and fluidity of PS vesicles upon contacting nanovesicles of different composition, were determined. This was followed by surveying the effect of injected or nebulized nanovesicles on the surface pressure of a PS monolayer in dynamic and static conditions.

The first finding was that no size change of PS vesicles occurred upon contact with nanovesicles. The size reduction of PS vesicles is associated to PS inactivation.[46,47] While large (in the order of several micrometres diameter) PS vesicles represent the surface-active components of PS, the smaller vesicles display slow adsorption and inability of reaching low surface tension.[46,47]Hydroxyapatite nanoparticles for instance, besides of changing the shape of compression isotherms, induce the size reduction of PS vesicles.[23] This fact is explained by the loss by partition of hydrophobic cationic proteins B and C[48,49] of the PS, on nanoparticles surface. B and C are transmembrane proteins that induce vesicle fusion to promote formation of large and surface-active vesicles. The loss of B and C proteins induces low surface pressure PS monolayers, since further adsorption/spreading of PS is impaired. Such proteins ensure an efficient re-extension of the interfacial film upon expansion essential for maintaining πe during inhalation[48] and are important for minimising the energy required to expand the alveolar interface and stabilise the lung epithelium. The size reduction of PS vesicles upon contacting deleterious agents is thus considered as a significant indication of surfactant degradation.[46,47] Here no changes in PS vesicles size were detected, suggesting that, different to rigid nanoparticles, no loss of hydrophobic proteins from PS vesicles was induced by contacting nanovesicles.

Despite of the lack of B and C losing however, a mutual structural perturbation between nanovesicles and PS vesicles was revealed. ApH for instance, slightly decreased the order of PS bilayers, while the order of ApH was significantly increased by PS vesicles. This suggested the occurrence of lipid exchange between PS vesicles and nanovesicles. According to the chemical nature of nanovesicles, such exchange may modify the fluidity and thus the tensioactive properties of the PS monolayer. Lipid monolayers that at body temperature are in liquid expanded (LE) phase such as DOPC under quasi elastic compression, collapse at πe. In contrast DPPC -the majoritary saturated phospholipid of PS- at 37 °C forms monolayers that under compression, convert from LE to tilted crystalline (TC) structures, and do not collapse above πe[20,51-54]. It was suggested thus that opposite to LE, the TC phase is needed to avoid monolayer collapse under compression.[55] In this context, fluidizing agents, namely lysoderivatives, fatty acids or unsaturated phospholipids (such as DOPE in pH-sensitive nanovesicles) may in one hand-and aided by B-C proteins[56] be required for normal PS spreading/adsorption[57]on the other, since fluidizing agents are LE phase inducers, may favour the collapse of a compressed monolayer.[29,51] Another example of the dual role played by fluidizing agents are lysoderivatives such as lysophosphatidylcholine, that form positively curved micelles that can prevent formation of HII structures by other lipids, inhibiting the adsorption of PS itself.[58] Summarizing, fluidizing agents actively inhibit the PS by multiple mechanisms.[17]We found however, that none nanovesicles (even the DOPE-containing pH-sensitive nanovesicles), increased the fluidity of PS vesicles. On the contrary, even the slight interaction with L decreased PS fluidity.

Interestingly, when injected in the subphase of PS monolayers compressed at 30 mN/m, nanovesicles affected the surface pressure along the subsequent expansion, that raised instead of decreasing to 0 mN/m. In particular, injected pH-sensitive nanovesicles shifted π from 0 to 25 mN/m (almost the 30 mN/m π value of the fully compressed PS monolayer alone). Such behaviour suggested not only absence of inactivation, but improvement of PS tensioactive

function. The highest increase of π was caused by pH-sensitive nanovesicles, structures that below pH 5.5- because of the CHEMS: DOPE content- experience a phase transition from lamellar to hexagonal HII.[59-61]The hexagonal HII phase is suggested to mediate the adsorption/fusion of bilayers without the surfactant proteins with monolayers in the interfase[58,62,63] and probably played a role in the interaction between ApH, LpH and PS monolayer. ARC on the other hand, affected π in the second expansion. ARC showed slower and less pronounced adsorption/fusion kinetics than pH-sensitive nanovesicles, probably because of the lack of HII phase, the same as L, that did not affect π during the two compression-expansions.

The PS inactivation caused by hydroxyapatite nanoparticles is described as a shift to the left of the π vs area isotherm.[23] In other words, the presence of inactivating nanoparticles counteracts the raise of π induced by compression. Here we showed that opposingly, pH-sensitive nanovesicles shifted the curve to the right: a slight compression induced higher π than in absence of nanovesicles. The increase of π would imply a reduction in the mechanical expansion effort during the inspiration. As discussed below, such encouraging results, not necessarily have a physiological parallel.

We finally compared the ability of injected vs nebulized nanovesicles to alter π of PS monolayers. Our results indicated that π was always increased according to the chemical nature, concentration, time of contact and route of administration of each nanovesicle. Nebulized nanovesicles caused the highest impact on π, at doses ~53 folds lower than injected in the subphase. The reason for this phenomenon lies in the disruptive effect of nebulization on the nanovesicle bilayer. Intact DPPC nanovesicles are known to slightly decrease the surface tension of water, in an extent depending on lipid processing.[64,65] That is because the monomeric phospholipids (the dominant surface tension lowering species) in equilibrium with aqueous dispersions of nanovesicles is extremely low between 10^{-8} -10^{-10} M.[64-69] The surface tension of the PS monolayer is only affected by nanovesicles in the subphase after diffusion and break open to render surface active lipid monomers that incorporate to the pre-existing monolayer.[70] Compared to non-pH-sensitive nanovesicles, subphase injected pH-sensitive nanovesicles increased π probably because of the better adsorption/spreading enabled by the HII-mediated stalk structure. The raise of π caused by subphase injection however, was slower and less pronounced compared to the induced by nebulization. This was probably owed to the shear stress of nebulization, responsible for generating surface active monomers. Recently, employing a closely related vibrating mesh nebulizer to the one used in [1] and in the present work, Stetten 2016[45]showed that nebulization of multilamellar vesicles of pure DPPC and of dimyristoylphosphatidylcholine shear opened the vesicles and created a high droplet surface area on which to store monomeric lipid.[45]The results discussed above however, were obtained on monolayers at 10 mN/m. When the surface pressure was increased to 30 mN/m the impact of nebulized nanovesicles on π was less pronounced, while at πe, nebulization did not affect it.

4 Conclusion

The conclusions arising from these simple experimental approaches can be grouped in three blocks: In the first one, we can state that at least a fraction of nebulized nanovesicles remained structurally stable after crossing a PS monolayer, retaining the ability of successfully executing cytoplasmic delivery. This would mean that therapeutic use of nebulized nanovesicles for targeted pH-sensitive cytoplasmic delivery is feasible, despite of being soft matter submitted to dismantling interactions (shear stress of nebulization and interaction with surfactant barrier) along the pathway to the underlying cells. In the second one, that nebulized nanovesicles can only increase the tensioactive function of a PS monolayer, when the monolayer is relaxed enough below πe, this is, out of the physiological range. This would mean that *in vivo*, perturbations on tensioactive function of the lung surfactant induced by nebulized nanovesicles, is poorly likely to occur. In the third one, that *in vivo*, though no monomer insertion in monolayer had taken place, the passage of nanovesicles across a PS monolayer may occur as well. The fact that cytoplasmic delivery from ApH slightly decreased across monolayers at πe, suggested that nanovesicles passage across PS monolayer was inversely related to monolayer compression during the respiratory cycle. This would mean that, while nebulized nanovesicles crossed the surfactant barrier with independence of monomers insertion, the cross would be dependent of the

compression degree of the monolayer. Together with the finding that nanovesicles neither depleted B and C proteins of the PS, not increased its fluidity, the results indicate that in our experimental conditions, nebulized nanovesicles would not induce biophysical changes leading to PS inactivation, opening the door to future deeper translational studies.

5 References

1. Rudokas M, Najlah M, Alhnan MA, Elhissi A. Liposome delivery systems for inhalation: a critical review highlighting formulation issues and anticancer applications. Medical Principles and Practice. 2016;25(2):60-72.
2. Cipolla D, Shekunov B, Blanchard J, Hickey A. Lipid-based carriers for pulmonary products: preclinical development and case studies in humans. Advanced drug delivery reviews. 2014;75:53-80.
3. Haque S, Whittaker MR, McIntosh MP, Pouton CW, Kaminskas LM. Disposition and safety of inhaled biodegradable nanomedicines: Opportunities and challenges. Nanomedicine: Nanotechnology, Biology and Medicine. 2016;12(6):1703-24.
4. Loira-Pastoriza C, Todoroff J, Vanbever R. Delivery strategies for sustained drug release in the lungs. Advanced drug delivery reviews. 2014;75:81-91.
5. Cipolla D, Redelmeier T, Eastman S, Bruinenberg P, Gonda I. Nanovesicles, niosomes and proniosomes–a critical update of their (commercial) development as inhaled products. Respiratory drug delivery Europe. 2011:41-54.
6. Sercombe L, Veerati T, Moheimani F, Wu SY, Sood AK, Hua S. Advances and challenges of liposome assisted drug delivery. Frontiers in pharmacology. 2015;6:286.
7. Sweeney S, Leo BF, Chen S, Abraham-Thomas N, Thorley AJ, Gow A, et al. Pulmonary surfactant mitigates silver nanoparticle toxicity in human alveolar type-I-like epithelial cells. Colloids and Surfaces B: Biointerfaces. 2016;145:167-75.
8. Clancy J, Dupont L, Konstan MW, Billings J, Fustik S, Goss CH, et al. Phase II studies of nebulisedArikace in CF patients with Pseudomonas aeruginosa infection. Thorax. 2013:thoraxjnl-2012-202-230.
9. Cipolla D, Blanchard J, Gonda I. Development of liposomal ciprofloxacin to treat lung infections. Pharmaceutics. 2016;8(1):6.
10. Altube MJ, Selzer SM, de Farias MA, Portugal RV, Morilla MJ, Romero EL. Surviving nebulization-induced stress: dexamethasone in pH-sensitive archaeosomes. Nanomedicine. 2016;11(16):2103-17.
11. Caimi AT, Parra F, de Farias MA, Portugal RV, Perez AP, Romero EL, et al. Topical vaccination with super-stable ready to use nanovesicles. Colloids and Surfaces B: Biointerfaces. 2016;152:114-23.
12. Greaves DR, Gordon S. The macrophage scavenger receptor at 30 years of age: current knowledge and future challenges. Journal of lipid research. 2009;50 (Supplement):S282-S6.
13. Niven RW, Schreier H. Nebulization of nanovesicles. I. Effects of lipid composition. Pharmaceutical research. 1990;7(11):1127-33.
14. List GR, King JW. Hydrogenation of Fats and Oils: Theory and Practice: Elsevier; 2016.
15. Hussell T, Bell TJ. Alveolar macrophages: plasticity in a tissue-specific context. Nature reviews immunology. 2014;14(2):81-93.
16. Possmayer F. Physicochemical aspects of pulmonary surfactant. Fetal and neonatal physiology. 2004;2:1014-34.
17. Lopez-Rodriguez E, Pérez-Gil J. Structure-function relationships in pulmonary surfactant membranes: from biophysics to therapy. Biochimica et Biophysica Acta (BBA)-Biomembranes. 2014;1838(6):1568-85.
18. Harishchandra RK, Saleem M, Galla H-J. Nanoparticle interaction with model lung surfactant monolayers. Journal of The Royal Society Interface. 2010;7(Suppl 1):S15-S26.
19. Schleh C, Hohlfeld JM. Interaction of nanoparticles with the pulmonary surfactant system. Inhalation toxicology. 2009;21(sup1):97-103.
20. Rugonyi S, Biswas SC, Hall SB. The biophysical function of pulmonary surfactant. Respiratory physiology & neurobiology. 2008;163(1):244-55.
21. Chhoden T, Clausen PA, Larsen ST, Nørgaard AW, Lauritsen FR. Interactions between nanoparticles and lung surfactant investigated by matrix-assisted laser desorption/ionization

time-of-flight mass spectrometry. Rapid Communications in Mass Spectrometry. 2015;29(11):1080-6.
22. Beck-Broichsitter M, Ruppert C, Schmehl T, Günther A, Seeger W. Biophysical inhibition of synthetic vs. naturally-derived pulmonary surfactant preparations by polymeric nanoparticles. Biochimica et Biophysica Acta (BBA)-Biomembranes. 2014;1838(1):474-81.
23. Fan Q, Wang YE, Zhao X, Loo JS, Zuo YY. Adverse biophysical effects of hydroxyapatite nanoparticles on natural pulmonary surfactant. ACS nano. 2011;5(8):6410-6.
24. Gonzalez RO, Higa LH, Cutrullis RA, Bilen M, Morelli I, Roncaglia DI, et al. Archaeosomes made of Halorubrumtebenquichense total polar lipids: a new source of adjuvancy. BMC biotechnology. 2009;9(1):71.
25. Kates M, Kushwaha S. Isoprenoids and polar lipids of extreme halophiles. Archaea, a laboratory manual Halophiles Cold Spring Harbor Laboratory Press, Cold Spring Harbor. 1995:35-54.
26. Böttcher C, Pries C. A rapid and sensitive sub-micro phosphorus determination. AnalyticaChimica Acta. 1961;24:203-4.
27. Higa LH, Schilrreff P, Perez AP, Iriarte MA, Roncaglia DI, Morilla MJ, et al. Ultradeformablearchaeosomes as new topical adjuvants. Nanomedicine: Nanotechnology, Biology and Medicine. 2012;8(8):1319-28.
28. A.A. Hager, T. DePaoli, US Pat., 6172203, 2001.
29. Lee S, Kim DH, Needham D. Equilibrium and dynamic interfacial tension measurements at microscopic interfaces using a micropipet technique. 2. Dynamics of Phospholipid Monolayer Formation and Equilibrium Tensions at the water− air interface. Langmuir. 2001;17(18):5544-50.
30. Gaines GL. Insoluble monolayers at liquid-gas interfaces. 1966.
31. Horie T, Hildebrandt J. Dynamic compliance, limit cycles, and static equilibria of excised cat lung. Journal of applied physiology. 1971;31(3):423-30.
32. Schürch S, Goerke J, Clements JA. Direct determination of volume-and time-dependence of alveolar surface tension in excised lungs. Proceedings of the National Academy of Sciences. 1978;75(7):3417-21.
33. Piknova B, Schram V, Hall S. Pulmonary surfactant: phase behavior and function. Current opinion in structural biology. 2002;12(4):487-94.
34. Zhang H, Wang YE, Fan Q. Zuo Y Y. On the low surface tension of lung surfactant. Langmuir. 2011; 27(13), 8351-8358.
35. Casals C, Cañadas O. Role of lipid ordered/disordered phase coexistence in pulmonary surfactant function. Biochimica et Biophysica Acta (BBA)-Biomembranes. 2012; 1818(11): 2550-2562.
36. Zuo YY, Veldhuizen RA, Neumann, AW, Petersen NO, Possmayer F. Current perspectives in pulmonary surfactant—inhibition, enhancement and evaluation. Biochimica et Biophysica Acta (BBA)-Biomembranes. 2008; *1778*(10):1947-1977.
37. Parasassi T, De Stasio G, Ravagnan G, Rusch R, Gratton E. Quantitation of lipid phases in phospholipid vesicles by the generalized polarization of Laurdan fluorescence. Biophysical journal. 1991;60(1):179-89.
38. Chong PL-G, Wong PT. Interactions of Laurdan with phosphatidylcholine nanovesicles: a high pressure FTIR study. Biochimica et Biophysica Acta (BBA)-Biomembranes. 1993;1149(2):260-6.
39. Sheffield MJ, Baker BL, Li D, Owen NL, Baker ML, Bell JD. Enhancement of Agkistrodonpiscivoruspiscivorus venom phospholipase A2 activity toward phosphatidylcholine vesicles by lysolecithin and palmitic acid: studies with fluorescent probes of membrane structure. Biochemistry. 1995;34(24):7796-806.
40. Harris FM, Smith SK, Bell JD. Physical properties of erythrocyte ghosts that determine susceptibility to secretory phospholipase A2. Journal of Biological Chemistry. 2001;276(25):22722-31.
41. Harris FM, Best KB, Bell JD. Use of laurdan fluorescence intensity and polarization to distinguish between changes in membrane fluidity and phospholipid order. Biochimica et Biophysica Acta (BBA)-Biomembranes. 2002;1565(1):123-8.
42. Wilson-Ashworth HA, Bahm Q, Erickson J, Shinkle A, Vu MP, Woodbury D, et al. Differential detection of phospholipid fluidity, order, and spacing by fluorescence spectroscopy of bis-pyrene, prodan, nystatin, and merocyanine 540. Biophysical journal. 2006;91(11):4091-101.
43. Carrer DC, Higa LH, Tesoriero MVD, Morilla MJ, Roncaglia DI, Romero EL. Structural features of ultradeformablearchaeosomes for topical delivery of ovalbumin. Colloids and Surfaces B: Biointerfaces. 2014;121:281-9.
44. Kitano T, Onoue T, Yamauchi K. Archaeal lipids forming a low energy-surface on air-water interface. Chemistry and physics of lipids. 2003;126(2):225-32.

45. Stetten AZ, Moraca G, Corcoran TE, Tristram-Nagle S, Garoff S, Przybycien TM, et al. Enabling Marangoni flow at air-liquid interfaces through deposition of aerosolized lipid dispersions. Journal of Colloid and Interface Science. 2016;484:270-8.
46. Velddhuizen RA, Li-Juan Y, Hearn SA, Possmayer F, Lewis JF. Surfactant-associated protein A is important for maintaining surfactant large-aggregate forms during surface-area cycling. Biochemical Journal. 1996;313(3):835-40.
47. Veldhuizen RA, Ito Y, Marcou J, Yao L, McCaig L, Lewis J. Effects of lung injury on pulmonary surfactant aggregate conversion in vivo and in vitro. American Journal of Physiology-Lung Cellular and Molecular Physiology. 1997;272(5):L872-L8.
48. Possmayer F, Nag K, Rodriguez K, Qanbar R, Schürch S. Surface activity in vitro: role of surfactant proteins. Comparative Biochemistry and Physiology Part A: Molecular & Integrative Physiology. 2001;129(1):209-20.
49. Rodriguez-Capote K, Nag K, Schürch S, Possmayer F. Surfactant protein interactions with neutral and acidic phospholipid films. American Journal of Physiology-Lung Cellular and Molecular Physiology. 2001;281(1):L231-L42.
50. Keating E, Zuo YY, Tadayyon SM, Petersen NO, Possmayer F, Veldhuizen RA (2012). A modified squeeze-out mechanism for generating high surface pressures with pulmonary surfactant. Biochimica et Biophysica Acta (BBA)-Biomembranes. 2012;1818(5), 1225-1234.
51. Gugliotti M, Politi MJ. The role of the gel liquid-crystalline phase transition in the lung surfactant cycle. Biophysical chemistry. 2001;89(2):243-51.
52. Clements JA. Functions of the Alveolar Lining 1, 2. American Review of Respiratory Disease. 1977;115(S):67-71.
53. Watkins J. The surface properties of pure phospholipids in relation to those of lung extracts. Biochimica et Biophysica Acta (BBA)-Lipids and Lipid Metabolism. 1968;152(2):293-306.
54. Bangham A, Morley C, Phillips M. The physical properties of an effective lung surfactant. Biochimica et Biophysica Acta (BBA)-Lipids and Lipid Metabolism. 1979;573(3):552-6.
55. Yan W, Biswas SC, Laderas TG, Hall SB. The melting of pulmonary surfactant monolayers. Journal of Applied Physiology. 2007;102(5):1739-45.
56. Lhert F, Yan W, Biswas SC, Hall SB. Effects of hydrophobic surfactant proteins on collapse of pulmonary surfactant monolayers. Biophysical journal. 2007;93(12):4237-43.
57. Notter R. Surface chemistry of pulmonary surfactant: the role of individual components. Elsevier, Amsterdam. 1984:17-53.
58. Biswas SC, Rananavare SB, Hall SB. Differential effects of lysophosphatidylcholine on the adsorption of phospholipids to an air/water interface. Biophysical journal. 2007;92(2):493-501.
59. Chu C-J, Dijkstra J, Lai M-Z, Hong K, Szoka FC. Efficiency of cytoplasmic delivery by pH-sensitive nanovesicles to cells in culture. Pharmaceutical research. 1990;7(8):824-34.
60. Venugopalan P, Jain S, Sankar S, Singh P, Rawat A, Vyas S. pH-sensitive nanovesicles: mechanism of triggered release to drug and gene delivery prospects. Die Pharmazie. 2002;57(10):659-71.
61. Andresen TL, Jensen SS, Jørgensen K. Advanced strategies in liposomal cancer therapy: problems and prospects of active and tumor specific drug release. Progress in lipid research. 2005;44(1):68-97.
62. Yu S-H, Harding PG, Possmayer F. Artificial pulmonary surfactant: Potential role for hexagonal hii phase in the formation of a surface-active monolayer. Biochimica et Biophysica Acta (BBA)-Biomembranes. 1984;776(1):37-47.
63. Perkins WR, Dause RB. Role of lipid polymorphism in pulmonary surfactant. Science. 1996;273(5273):330.
64. Kim SH, Franses EI. New protocols for preparing dipalmitoylphosphatidylcholine dispersions and controlling surface tension and competitive adsorption with albumin at the air/aqueous interface. Colloids and Surfaces B: Biointerfaces. 2005;43(3):256-66.
65. Wen X, Franses EI. Role of subsurface particulates on the dynamic adsorption of dipalmitoylphosphatidylcholine at the air/water interface. Langmuir. 2001;17(11):3194-201.
66. Buboltz JT, Feigenson GW. Phospholipid solubility determined by equilibrium distribution between surface and bulk phases. Langmuir. 2005;21(14):6296-301.
67. Kim SH, Haimovich-Caspi L, Omer L, Talmon Y, Franses EI. Effect of sonication and freezing–thawing on the aggregate size and dynamic surface tension of aqueous DPPC dispersions. Journal of colloid and interface science. 2007;311(1):217-27.

68. Smith R, Tanford C. The critical micelle concentration of l-α-dipalmitoylphosphatidylcholine in water and water/methanol solutions. Journal of molecular biology. 1972;67(1):75-83.
69. Marsh D, King MD. Prediction of the critical micelle concentrations of mono-and di-acyl phospholipids. Chemistry and physics of lipids. 1986;42(4):271-7.
70. Launois-Surpas M, Ivanova T, Panaiotov I, Proust J, Puisieux F, Georgiev G. Behavior of pure and mixed DPPC nanovesicles spread or adsorbed at the air-water interface. Colloid & Polymer Science. 1992;270(9):901-11.

Table 1: Structural features of nanovesicles and PS vesicles

Sample	Mean Diameter (nm ± SD)	pdi	ζ Potential (mV ± SD)	Total Lipids (mg/ml ± SD)
L	271 ± 45	0.37 ± 0.08	-6.6 ± 0.8	5.6 ± 1.7
ARC	179 ± 49	0.25 ± 0.06	-39.1 ± 7.1	7.2 ± 2.2
LpH	188 ± 18	0.22 ± 0.0	-20.2 ± 9.2	4.5 ± 2.2
ApH	174 ± 48	0.49 ± 0.33	-30.7 ± 13.0	6.0 ± 1.4
PS	1057 ± 293	0.64 ± 0.18	-20.5 ± 7.6	30 ± 2.5

Data are expressed as mean ± SD from three independent batches. PDI: Polydispersity index; SD: Standard deviation.

Table 2: HPTS encapsulated in nanovesicles 3 hours after post nanovesicles nebulization on PS monolayer covering J774A.1 cells.

Cell Supernatant	Surface Pressure (mN/m)	Encapsulated HPTS (%)
L	0	47.7 ± 0.1*
	10	55.7 ± 1.9
	45	61.7 ± 4.9
ARC	0	58.9 ± 3.9
	10	47.5 ± 8.1**
	45	55.5 ± 1.5
LpH	0	69.2 ± 4.6
	10	67.5 ± 2.5
	45	63.0 ± 1.3
ApH	0	74.2 ± 6.4
	10	77.0 ± 1.1
	45	75.2 ± 3.6

Data are expressed as mean ± SD.

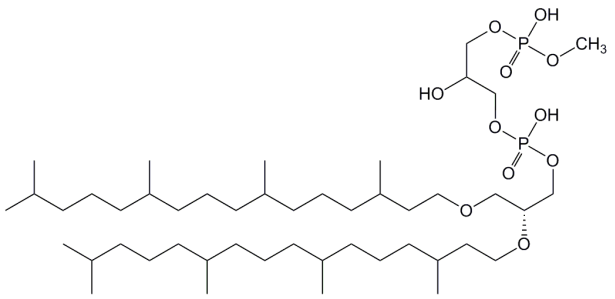

Figure 1: Chemical structure of 2,3-di-O-phytanyl-sn-glycero-1-phospho-(3'-sn-glycerol-1'-methyl phosphate) (PGP-Me), main polar archaeolipid from *H. tebenquichense.* The PGP-Me is recognized as a ligand by Scavenger Receptor Class A in macrophages[10].

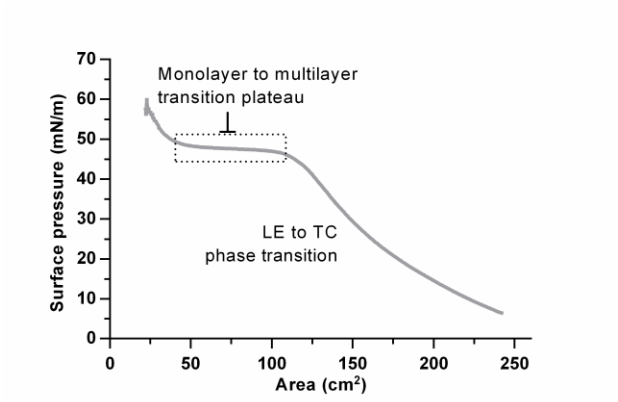

Figure 2: A compression isotherm of Prosurf monolayer. As the surface pressure increases from 10 mN/m to 40 mN/m, a LE- TC phase transition occurs, characterized by a plateau between 40 mN/m to 50 mN/m where TC and LE domains coexist, known as the equilibrium surface pressure πe. Further compression above πe increased the surface pressure of the monolayer; in this condition, the interfacial PS monolayer interacts with squeezed out bilayers[35,36] until collapsing at 60 mN/m.

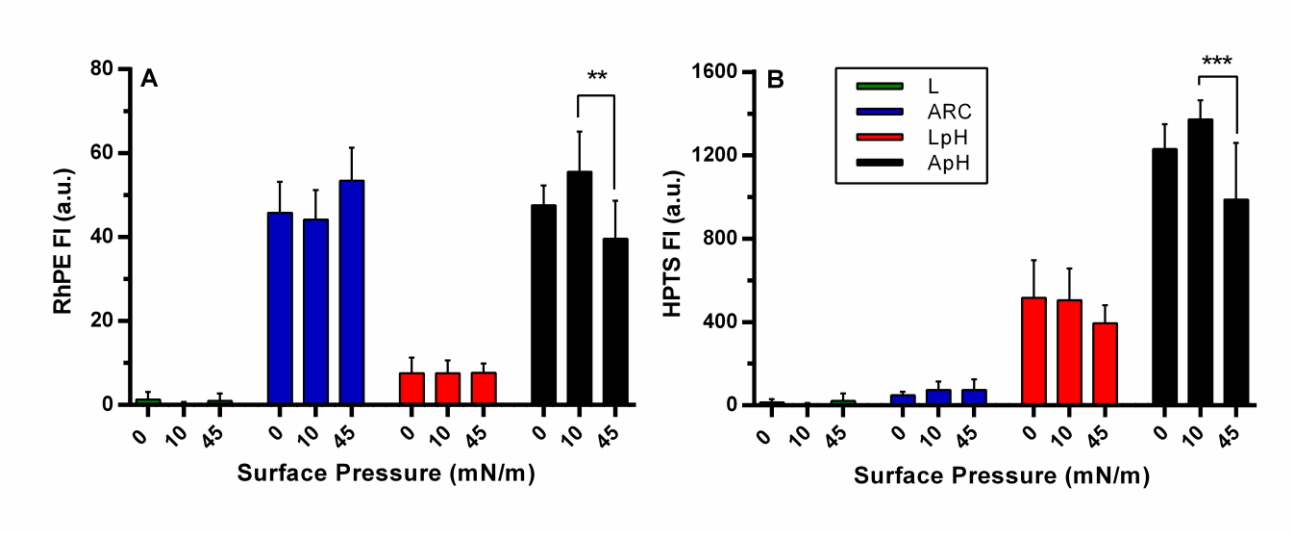

Figure 3: Fluorescence Intensity from RhPE (a) and HPTS (b) inside J774A.1 cells, 3 hours post nanovesicles nebulization. Before nebulization, each well was covered with PS amounts roughly corresponding to 10 or 45 mN/m surface pressure, according to the lipid mass/area ratio previously determined in the compression isotherm of Prosurf.

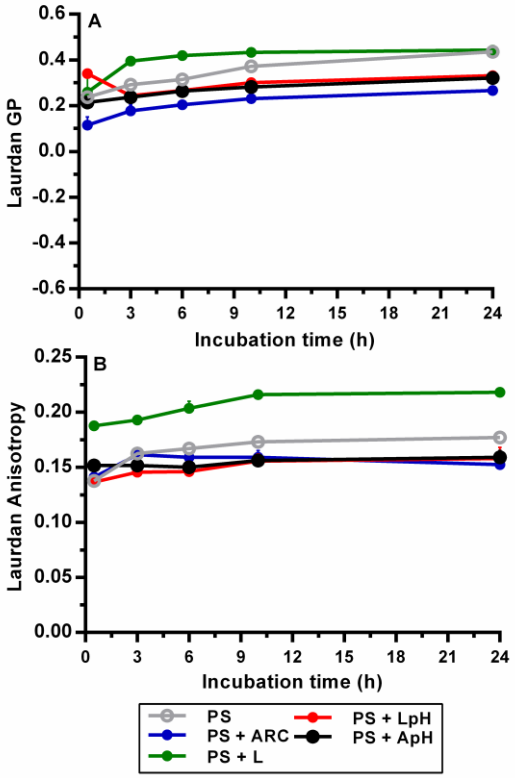

Figure 4: Laurdan Generalized Polarization (GP) (a) and Fluorescence Anisotropy (b) in PS vesicles alone and after contacting nanovesicles as a function of time.

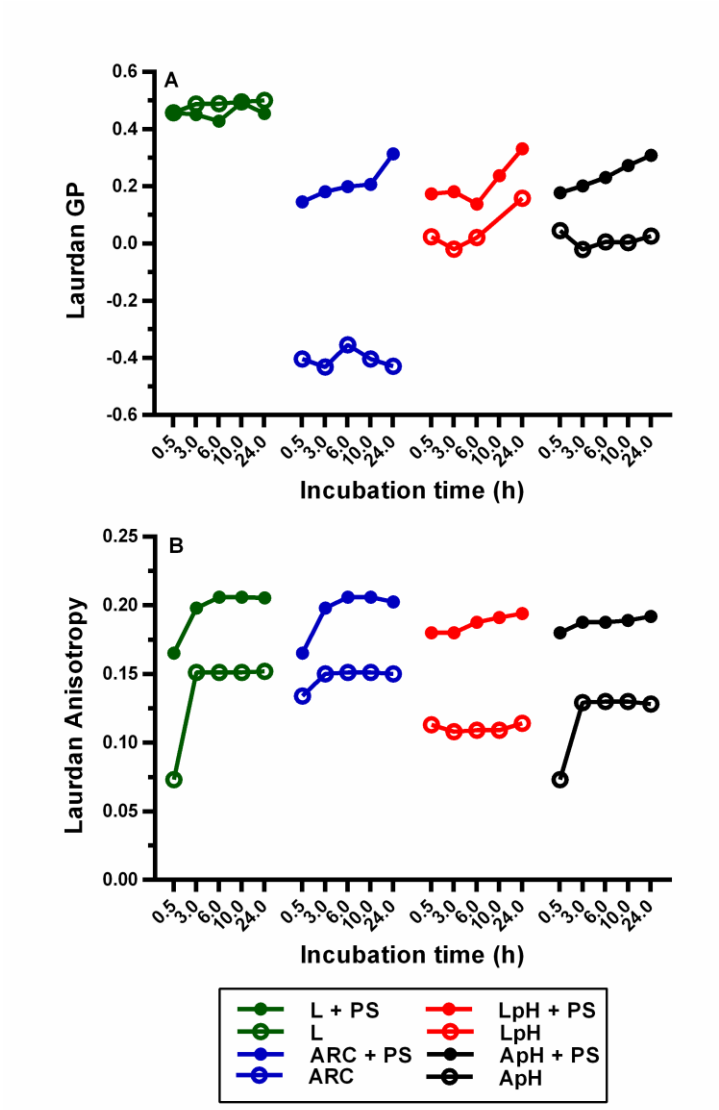

Figure 5: Laurdan Generalized Polarization (GP) (a) and Fluorescence Anisotropy (b) in nanovesicles alone and after contacting PS vesicles as a function of time.

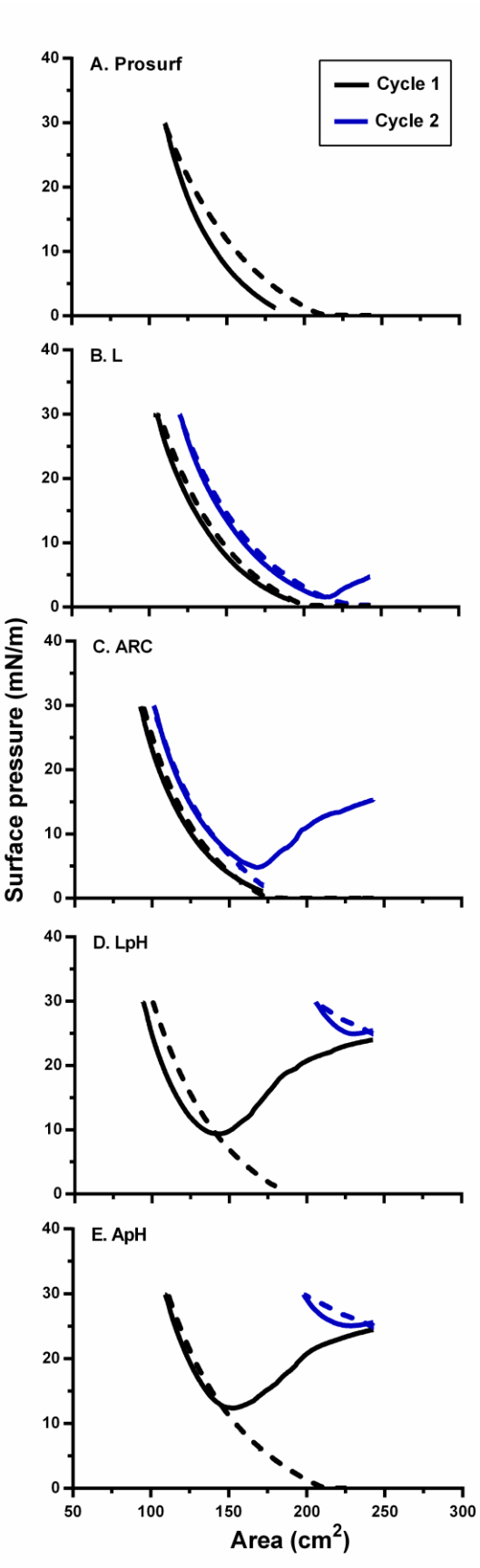
A. Prosurf
Cycle 1
Cycle 2
B. L
C. ARC
D. LpH
E. ApH
Surface pressure (mN/m)
Area (cm2)
0
10
20
30
40
50
100
150
200
250
300

Figure 6: Compression-expansion isotherms of PS. Nanovesicles were injected in the subphase in the first compression at 30 mN/m surface pressure. Continuous line: expansion, dot line: compression.

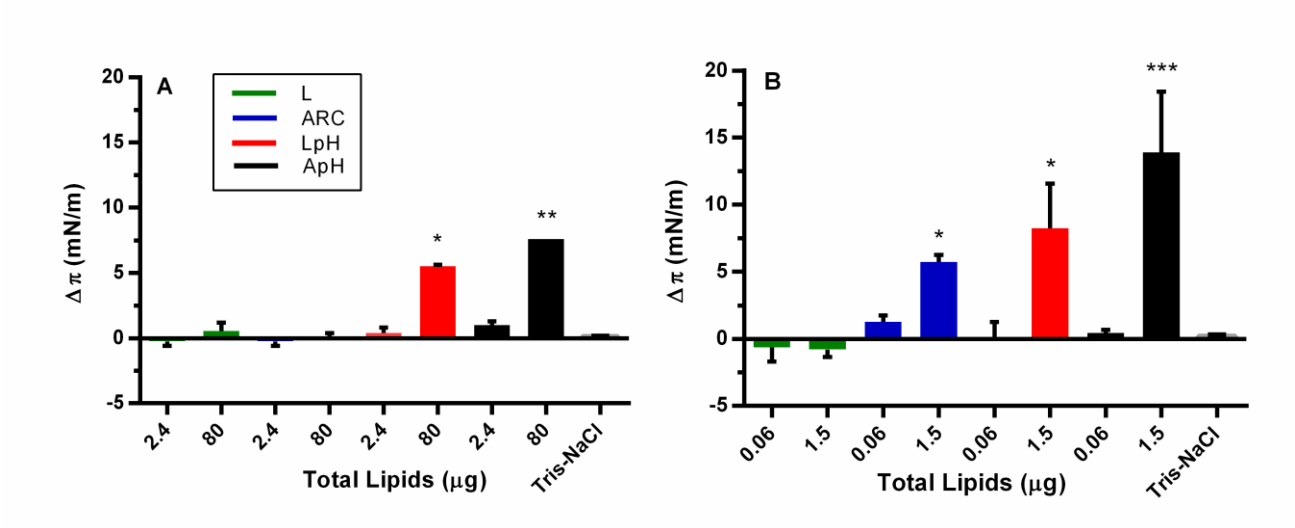

Figure 7: Variation ($\Delta\pi$) in PS monolayer surface pressure after 15 minutes the nanovesicles were (a) injected in the aqueous subphase or (b) nebulized. $\Delta\pi=\pi_{final}-\pi_{initial}$, with $\pi_{initial}$= 10 mN/m.

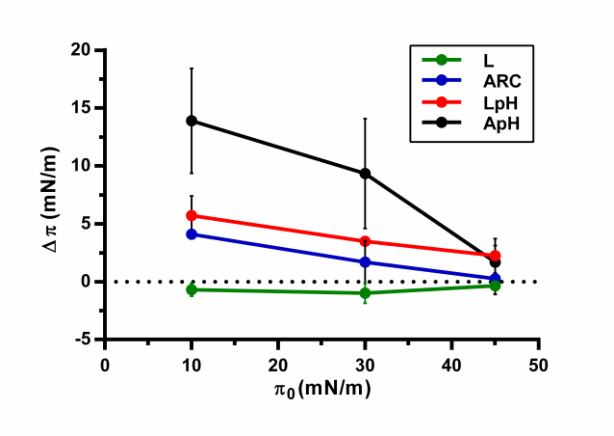

Figure 8: Variation ($\Delta\pi$) in PS monolayer surface pressure 15 minutes after the nanovesicles were nebulized. $\Delta\pi=\pi_{final}-\pi_{initial}$, with $\pi_{initial}$= 10, 30 and 45 mN/m.

.